



Published in final edited form as:

Org Lett. 2016 August 5; 18(15): 3902–3905. doi:10.1021/acs.orglett.6b01936.

## Thermodynamic and Structural Impact of $\alpha,\alpha$ -Dialkylated Residue Incorporation in a $\beta$ -Hairpin Peptide

Megan A. Karnes<sup>§,†</sup>, Shelby L. Schettler<sup>§,†</sup>, Halina M. Werner<sup>‡</sup>, Alana F. Kurz<sup>‡</sup>, W. Seth Horne<sup>‡</sup>, and George A. Lengyel<sup>†,\*</sup>

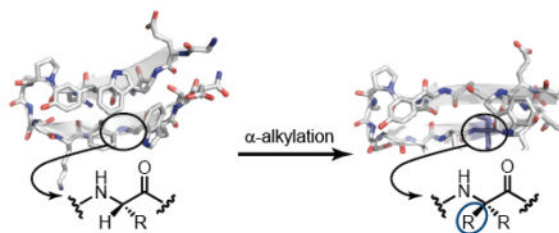
<sup>†</sup>Department of Chemistry, Slippery Rock University, Slippery Rock, Pennsylvania 16057, United States

<sup>‡</sup>Department of Chemistry, University of Pittsburgh, Pittsburgh, Pennsylvania 15260, United States

### Abstract

Peptides containing  $\alpha,\alpha$ -dialkylated  $\alpha$ -amino acids, owing to their ability to disrupt aggregation of  $\beta$ -amyloid proteins, have therapeutic potential in the treatment of neurodegenerative diseases. Thermodynamic and structural analyses are reported for a series of  $\beta$ -hairpin peptides containing  $\alpha,\alpha$ -dialkylated  $\alpha$ -amino acids with varying side-chain lengths. Results of these experiments show that  $\alpha,\alpha$ -dialkylated  $\alpha$ -amino acids with side-chain lengths longer than one carbon unit are tolerated in a  $\beta$ -hairpin, although at a moderate cost to folded stability.

### Graphical Abstract



$\alpha$ -Amino acids bearing two alkyl substituents at  $C_\alpha$  are common building blocks in peptide-based natural products<sup>1–3</sup> as well as synthetic peptidomimetics.<sup>4</sup>  $\alpha$ -Aminoisobutyric acid (Aib, Figure 1), the most well-studied  $\alpha,\alpha$ -dialkylated  $\alpha$ -amino acid, strongly promotes helical secondary structures<sup>5</sup> and can act as a “ $\beta$ -breaker,” significantly disfavoring  $\beta$ -sheet formation.<sup>6</sup> In cases where Aib has been examined in sheet secondary structure contexts, it can also act as a tight turn inducer.<sup>7,8</sup> Chiral  $C_\alpha$ -Me-residues are also excellent helix

\*Corresponding Author: george.lengyel@sru.edu.

#### §Author Contributions

These authors contributed equally.

#### Notes

The authors declare no competing financial interests.

#### Supporting Information

The Supporting Information is available free of charge on the ACS Publications website. Experimental methods, supplemental figures, supplemental tables (PDF)

stabilizers, even when the parent  $\alpha$ -amino acid typically favors sheet (e.g., ( $\alpha$ Me)Val vs. Val).<sup>9</sup> In contrast to Aib and related ( $\alpha$ Me) $\alpha$ -residues, a number of symmetric  $\alpha,\alpha$ -dialkylated  $\alpha$ -amino acids bearing bulkier substituents can promote fully-extended backbone conformations.<sup>10</sup> For example, small homooligomers of diethylglycine (Deg) and di-*n*-propylglycine (Dp<sub>*n*g</sub>) have been shown to form fully-extended chains both in solution and the solid state.<sup>11–15</sup> Seeking to leverage this precedent toward biomedical application, recent studies have shown that strategic incorporation of bulky  $\alpha,\alpha$ -dialkylated amino acids (e.g., diisobutylglycine, dibenzylglycine, di-*n*-propylglycine) into short  $\beta$ -strands can cap growing  $\beta$ -sheets, preventing formation of amyloid fibrils and even promoting their disassembly.<sup>16–18</sup>

While the structural studies described above indicate that  $\alpha,\alpha$ -dialkylated  $\alpha$ -amino acids can promote extended conformations in peptides, the thermodynamic impact of such modifications in the biologically relevant context of aqueous medium has not been investigated. Addressing this gap in knowledge would improve fundamental understanding of the role of  $\alpha,\alpha$ -dialkylated  $\alpha$ -amino acid side-chain identity in promoting  $\beta$ -sheet folds. Such knowledge, in turn, could enable applications related to amyloid inhibition by identifying residues that not only promote folding and facilitate tight binding to the exposed end of a  $\beta$ -sheet but also prevent the next strand from docking to the growing aggregate. Based on the precedent detailed above, we hypothesized that side-chain steric bulk could be optimized to achieve this end. Thus, we set out in the present work to systematically examine the structural and thermodynamic consequences of incorporation of four different achiral symmetric  $\alpha,\alpha$ -dialkylated  $\alpha$ -residues (Figure 1) in the context of a  $\beta$ -hairpin fold.

We chose peptide **1a** (Figure 2) as a host in which to explore the above questions. This 16-residue sequence (Figure 2a), derived from the C-terminal hairpin of protein GB1,<sup>19,20</sup> consists of two anti-parallel  $\beta$ -strands connected by a four-residue (PATG) turn. All modifications to **1a** were made at Ala<sup>13</sup>, the central residue in the C-terminal strand of the  $\beta$ -hairpin. This position was selected based on two lines of reasoning. First, because Ala<sup>13</sup> is at a non-hydrogen-bonding site, substitution with dialkylated  $\alpha$ -residues will not disrupt intrastrand backbone interactions necessary for folding; this increases the relevance of results to inform the use of dialkylated residues to disrupt  $\beta$ -sheet-mediated aggregation. Second, modifications to the side chain at Ala<sup>13</sup> will not alter the hydrophobic core of the folded hairpin consisting of residues Trp<sup>3</sup>, Tyr<sup>5</sup>, Phe<sup>12</sup>, and Val<sup>14</sup>.

In order to systematically probe the relationship between steric bulk in  $\alpha,\alpha$ -dialkylated  $\alpha$ -residues and  $\beta$ -sheet forming propensity, we synthesized the series of peptides **1b–4b** (Figure 2b). These sequences incorporate one of four  $\alpha,\alpha$ -dialkylated  $\alpha$ -residues in place of Ala<sup>13</sup> in **1a**: Aib in **1b**, diethylglycine (Deg) in **2b**, di-*n*-propylglycine (Dp<sub>*n*g</sub>) in **3b**, and di-*n*-butylglycine (Db<sub>*n*g</sub>) in **4b**. To isolate any effects of increasing side-chain length and hydrophobicity on folding, we prepared additional control sequences where Ala<sup>13</sup> was replaced with monoalkylated residues  $\alpha$ -aminobutyric acid (**2a**), norvaline (**3a**), or norleucine (**4a**). Peptides **2a–4a** and **1b–4b** were synthesized using standard Fmoc solid-phase methods, purified by preparative HPLC, and the identity and purity of each sequence confirmed by MALDI-MS and analytical HPLC (see Supporting Information).

We first assessed the folding behavior of control peptides **1a–4a** by multidimensional NMR (TOCSY, NOESY, and COSY) at 278 K in 50 mM phosphate buffer (9:1 H<sub>2</sub>O/D<sub>2</sub>O, pH 6.3 uncorrected for presence of D<sub>2</sub>O). Spectral data for peptide **1a** were previously reported under identical conditions.<sup>20</sup> The magnitude of chemical shift separation ( $\delta$ ) between the two diastereotopic protons found in glycine residues near the turn of a  $\beta$ -hairpin-forming peptide can be used as a spectroscopic handle to quantify folded population.<sup>22</sup> Thus, we assigned the chemical shifts of the H<sub>N</sub> and H <sub>$\alpha$</sub>  resonances from Gly<sup>10</sup> in **1a–4a** (Table S2) and used these data to calculate the  $\delta$  and folded population for each sequence. A reference  $\delta$  value of 0.310 ppm was used for the fully folded state in these calculations based on data previously reported for a disulfide-cyclized variant of **1a**.<sup>20</sup> The folded populations and corresponding  $G_{\text{fold}}$  values for peptides **1a–4a** are identical within experimental uncertainty (Table 1). These data indicate that, despite increasing relative hydrophobicity of the residues in question, increasing the length of the side chain at position 13 in this peptide sequence has little or no impact on  $\beta$ -hairpin folded stability.

We next examined the peptide series **1b–4b** under identical conditions. We noted poor solubility of these peptides at 278 K, which we attribute to the added hydrophobicity from the  $\alpha,\alpha$ -dialkylated  $\alpha$ -residues at a solvent-exposed position in the hairpin. At a higher temperature of 298 K, the samples were fully homogeneous and spectra showed clear splitting of H<sub>N</sub> resonances (Figure S1), supporting the absence of aggregation. Thus, we proceeded with the analysis of folded population based on glycine H <sub>$\alpha$</sub>  chemical shifts at the higher temperature (Table 1). Previously reported data are provided for peptide **1a** at 293 K to facilitate comparison.<sup>20</sup>

The NMR data for **1b–4b** support the hypothesis that increasing steric bulk in the dialkylated  $\alpha$ -residue beyond the size of a methyl group shifts the equilibrium to favor sheet secondary structure. As expected, substitution of Ala<sup>13</sup> in **1a** with Aib in **1b** almost completely abolishes the  $\beta$ -hairpin fold. Replacing the Aib in **1b** with Deg in **2b** boosts the folded population to ~26%. Interestingly, increasing the steric bulk beyond Deg in **2b** to Dpg in **3b** and Dbg in **4b** had no additional effect on folded population. In all cases, the folds of peptides bearing alkylated residues are destabilized relative to control peptide **1a**. This destabilization may be caused by a loss of chirality in the backbone; in a recent study carried out in the context of a helix in a small protein, it was demonstrated that such a loss of chirality can lead to an entropic destabilization of the folded state.<sup>23</sup>

Collectively, the NMR data obtained for **1b–4b** show that (1) consistent with precedent, the dialkylated  $\alpha$ -amino acid Aib is a strong sheet breaker; (2) extending the size of the side chain from methyl to ethyl partially mitigates this effect; (3) increasing the size of the linear dialkylated side chain beyond two carbon units has no measurable impact on folding; and (4) none of the dialkylated  $\alpha$ -residues promote sheet formation as effectively as a protein  $\alpha$ -amino acid. These results are in line with previously published conformational studies of homopolymers comprised of  $\alpha,\alpha$ -dialkylated  $\alpha$ -amino acids.<sup>10,24,25</sup>

One possible origin of the destabilization seen in peptides **2b–4b** is that the folded structure in these sequences is fundamentally different than that of the host  $\beta$ -hairpin. In order to test this hypothesis, we pursued the high-resolution structure of a hairpin bearing an  $\alpha,\alpha$ -

dialkylated  $\alpha$ -residue. The low folded populations of peptides **2b–4b** under conditions in which they were soluble precluded direct structural analysis. In order to circumvent this issue, we made mutations elsewhere in the sequence to further stabilize the hairpin fold. It has been shown that introducing a “tryptophan zipper” motif into sequences similar to **1a** dramatically increases the folded stability of the  $\beta$ -hairpin.<sup>26</sup> Thus, we prepared peptide **5a** (Figure 2), which contains a Val<sup>14</sup>-to-Trp mutation relative to **1a**, and peptide **5b**, which contains the same Val<sup>14</sup>-to-Trp mutation in the context of Deg-containing sequence **2b**. As there was no significant difference between the folded populations of peptides containing Deg, Dp<sub>ng</sub>, or Db<sub>ng</sub>, we anticipated results for Deg would prove broadly informative.

We carried out multidimensional NMR on peptides **5a** and **5b** at 298 K and assigned the backbone (Tables S3, S4) and side-chain resonances for each. Glycine diastereotopic H <sub>$\alpha$</sub>  chemical shifts (Table 1) suggested that the folded population of **5a** was indistinguishable from that of a disulfide-cyclized variant of **1a** reported in a previous study.<sup>20</sup> This result shows that the introduction of tryptophan at position 14 had the intended stabilizing effect. The corresponding analysis of peptide **5b** indicated a folded population of 49%, a significant increase relative to peptide **2b**. The fact that Val<sup>14</sup>-to-Trp substitution had the same apparent stabilizing effect on **1a** and **2b** supports the hypothesis that these two peptides (as well as **5a** and **5b**) adopt similar hairpin folds. To provide more direct evidence bearing on this question, we examined the folded structures of **5a** and **5b** through detailed NOE analysis. Overlap of side-chain resonances prevented unambiguous assignment of some NOEs; however, we were able to locate several long-range contacts in both sequences consistent with the expected  $\beta$ -hairpin folded conformation (Figure 3).

Encouraged by these results, we carried out simulated annealing with NMR-derived distance restraints to calculate high-resolution folded structures of **5a** and **5b**.<sup>27,28</sup> For each peptide, we used unambiguous NOE signals to tabulate a set of inter-residue distance restraints (Tables S5, S6). These restraints were used to generate ensembles of three-dimensional structures which converged to  $\beta$ -hairpin conformations for both peptides (Figure S4). After confirming the hydrogen-bond register for **5a** and **5b** in preliminary simulations, we added additional distance restraints to enforce the corresponding inter-strand hydrogen bonds and generated new ensembles. We used the ten lowest energy structures from each ensemble (Figure S5) to calculate average NMR structures for the two peptides (Figure 4).

The NMR structures show that **5a** and **5b** both adopt similar canonical  $\beta$ -hairpin folds. Despite destabilization caused by inclusion of the  $\alpha,\alpha$ -dialkylated  $\alpha$ -residue, the folded state of **5b** appears very similar to that of peptide **5a**. For comparison of these hairpins to a typical protein  $\beta$ -sheet, we calculated root-mean square deviation (RMSD) values for the backbone overlay of peptides **5a** and **5b** to the C-terminal hairpin of protein GB1, the origin of sequence **1a** (Figure S6).<sup>21</sup> Both natural peptide **5a** and variant **5b** bearing a Deg residue aligned well with the full length protein (RMSD 0.866 Å and 1.347 Å, respectively). That fact that the RMSD values for the two sequences are similar indicates that the presence of the  $\alpha,\alpha$ -dialkylated  $\alpha$ -residue, while energetically destabilizing, does not significantly perturb the  $\beta$ -hairpin fold.

In summary, we have shown for first time the thermodynamic consequences of incorporating  $\alpha,\alpha$ -dialkylated  $\alpha$ -amino acids into a  $\beta$ -sheet context in aqueous medium. Symmetric  $\alpha,\alpha$ -dialkylated  $\alpha$ -amino acids with linear side chains can be accommodated into a  $\beta$ -hairpin secondary structure, albeit with accompanying destabilization of the folded structure, potentially limiting therapeutic efficacy in peptides containing these residues. The possibility exists that further fine-tuning of side chain structure may minimize this destabilization or perhaps even reverse it. We hypothesize that these ends may be achieved by examining chiral  $\alpha,\alpha$ -dialkylated  $\alpha$ -residues or by utilizing more diverse side chains; homopolymers of  $\beta$ -branched  $\alpha,\alpha$ -dialkylated  $\alpha$ -amino acids, for example, have shown the ability to template sheet formation.<sup>29</sup> Work towards these ends is ongoing.

## Supplementary Material

Refer to Web version on PubMed Central for supplementary material.

## Acknowledgments

This work was funded by Slippery Rock University and by the National Institutes of Health (R01GM107161 to W.S.H.).

## References

1. Duclohier H. *Chem Biodivers.* 2007; 4:1023. [PubMed: 17589874]
2. Toniolo C, Brückner H. *Chem Biodiv.* 2007; 4:1021.
3. Brückner H, Toniolo C. *Chem Biodiv.* 2013; 10:731.
4. Benedetti E. *Biopolymers.* 1996; 40:3. [PubMed: 8541447]
5. Karle IL, Balaram P. *Biochemistry.* 1990; 29:6747. [PubMed: 2204420]
6. Moretto V, Crisma M, Bonora GM, Toniolo C, Balaram H, Balaram P. *Macromolecules.* 1989; 22:2939.
7. Aravinda S, Shamala N, Balaram P. *Chem Biodiv.* 2008; 5:1238.
8. Wu L, McElheny D, Setnicka V, Hilario J, Keiderling TA. *Proteins: Struct, Funct, Bioinf.* 2012; 80:44.
9. Valle G, Crisma M, Toniolo C, Polinelli S, Boesten WHJ, Schoemaker HE, Meijer EM, Kamphuis J. *Int J Pept Protein Res.* 1991; 37:521. [PubMed: 1917310]
10. Peggion C, Moretto A, Formaggio F, Crisma M, Toniolo C. *Biopolymers.* 2013; 100:621. [PubMed: 23893391]
11. Toniolo C, Benedetti E. *Macromolecules.* 1991; 24:4004.
12. Toniolo C, Bonora GM, Bavoso A, Benedetti E, Di Blasio B, Pavone V, Pedone C, Barone V, Lelj F, Leplawy MT, Kaczmarek K, Redlinski A. *Biopolymers.* 1988; 27:373.
13. Benedetti E, Di Blasio B, Pavone V, Pedone C, Bavoso A, Toniolo C, Bonora GM, Leplawy MT, Hardy PM. *J Biosci.* 1985; 8:253.
14. Barone V, Lelj F, Bavoso A, Di Blasio B, Grimaldi P, Pavone V, Pedone C. *Biopolymers.* 1985; 24:1759.
15. Bonora GM, Toniolo C, Di Blasio B, Pavone V, Pedone C, Benedetti E, Lingham I, Hardy P. *J Am Chem Soc.* 1984; 106:8152.
16. Etienne MA, Aucoin JP, Fu Y, McCarley RL, Hammer RP. *J Am Chem Soc.* 2006; 128:3522. [PubMed: 16536517]
17. Bett CK, Ngunjiri JN, Serem WK, Fontenot KR, Hammer RP, McCarley RL, Garno JC. *ACS Chem Neurosci.* 2010; 1:608. [PubMed: 22778850]

18. Bett CK, Serem WK, Fontenot KR, Hammer RP, Garno JC. ACS Chem Neurosci. 2010; 1:661. [PubMed: 22778807]
19. Fesinmeyer RM, Hudson FM, Andersen NH. J Am Chem Soc. 2004; 126:7238. [PubMed: 15186161]
20. Lengyel GA, Horne WS. J Am Chem Soc. 2012; 134:15906. [PubMed: 22946450]
21. Frericks Schmidt HL, Sperling LJ, Gao YG, Wylie BJ, Boettcher JM, Wilson SR, Rienstra CM. J Phys Chem B. 2007; 111:14362. [PubMed: 18052145]
22. Fesinmeyer RM, Hudson FM, Olsen K, White GN, Euser A, Andersen N. J Biomol NMR. 2005; 33:213. [PubMed: 16341751]
23. Tavenor NA, Reinert ZE, Lengyel GA, Griffith BD, Horne WS. Chem Commun. 2016; 52:3789.
24. Toniolo C, Crisma M, Formaggio F, Peggion C. Biopolymers. 2001; 60:396. [PubMed: 12209474]
25. Tanaka M. Chem Pharm Bull. 2007; 55:349. [PubMed: 17329870]
26. Cochran AG, Skelton NJ, Starovasnik MA. Proc Natl Acad Sci USA. 2001; 98:5578. [PubMed: 11331745]
27. Brunger AT, Adams PD, Clore GM, DeLano WL, Gros P, Grosse-Kunstleve RW, Jiang J-S, Kuszewski J, Nilges M, Pannu NS, Read RJ, Rice LM, Simonson T, Warren GL. Acta Crystallogr Sect D: Biol Crystallogr. 1998; 54:905. [PubMed: 9757107]
28. Brunger AT. Nat Protoc. 2007; 2:2728. [PubMed: 18007608]
29. De Simone G, Lombardi A, Galdiero S, Nastri F, Di Costanzo L, Gohda S, Sano A, Yamada T, Pavone V. Biopolymers. 2000; 53:182. [PubMed: 10679622]

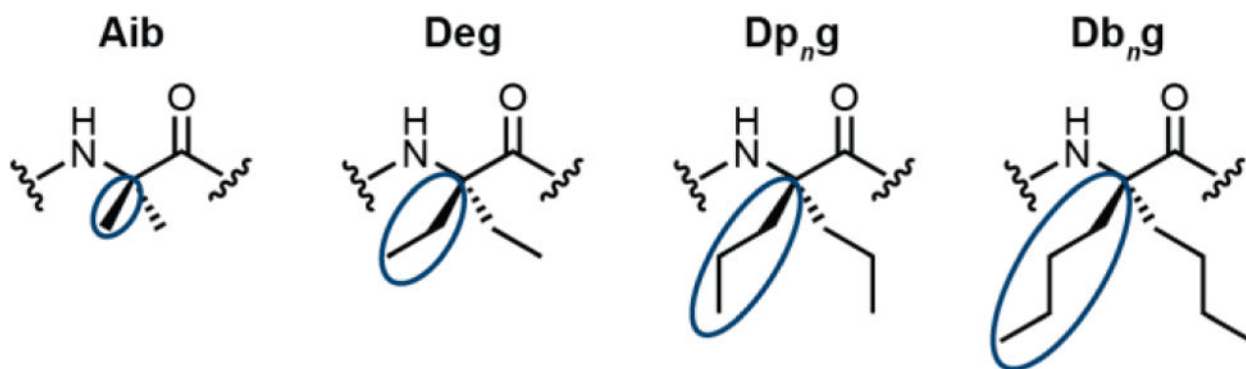


**Figure 1.**

Examples of symmetric  $\alpha,\alpha$ -dialkylated  $\alpha$ -residues:  $\alpha$ -aminoisobutyric acid (Aib), diethylglycine (Deg), di-*n*-propylglycine ( $Dp_n g$ ), and di-*n*-butylglycine ( $Db_n g$ ). The additional side chains of the  $\alpha,\alpha$ -dialkylated  $\alpha$ -amino acids are circled.

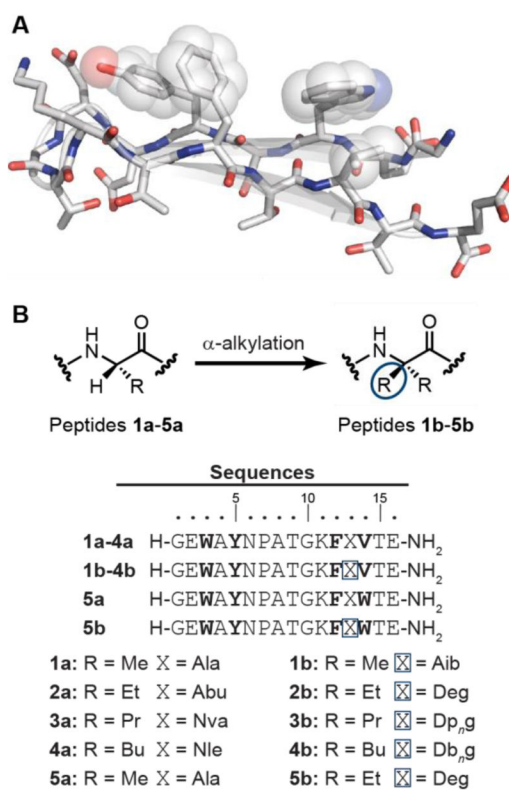


**Figure 2.**  
**(A)** Folded structure of the C-terminal hairpin from protein GB1 (PDB: 2QMT).<sup>21</sup> Side chains of hydrophobic core residues are indicated with spheres. **(B)** Sequences of peptides **1a-5a** and **1b-5b**.  $\alpha,\alpha$ -Dialkylated  $\alpha$ -residues are indicated with blue boxes and the hydrophobic core in bold.



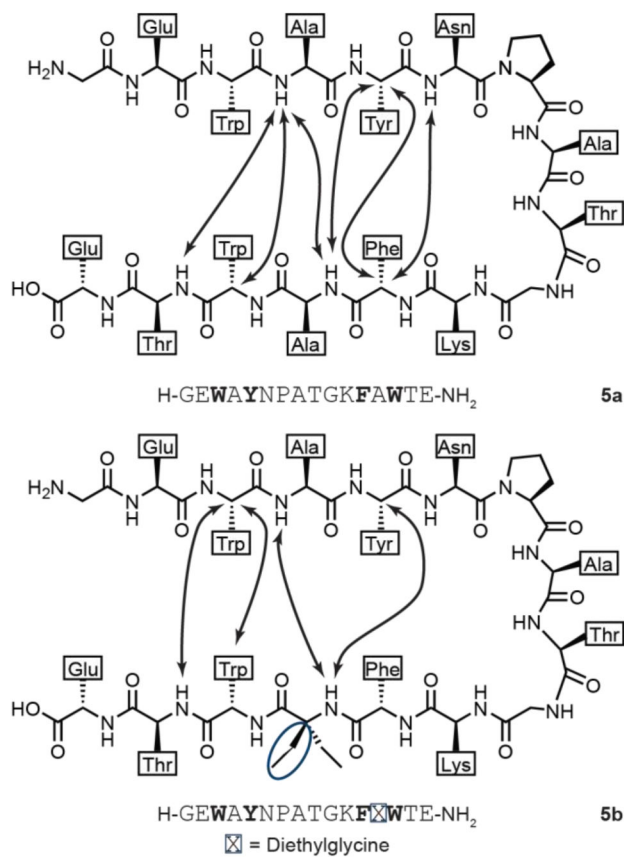


**Figure 3.** NOE analysis of peptides **5a** and **5b**. Arrows indicate the presence of cross-strand NOEs consistent with a  $\beta$ -hairpin folded conformation. The additional side chain of the  $\alpha,\alpha$ -dialkylated  $\alpha$ -amino acid is circled.

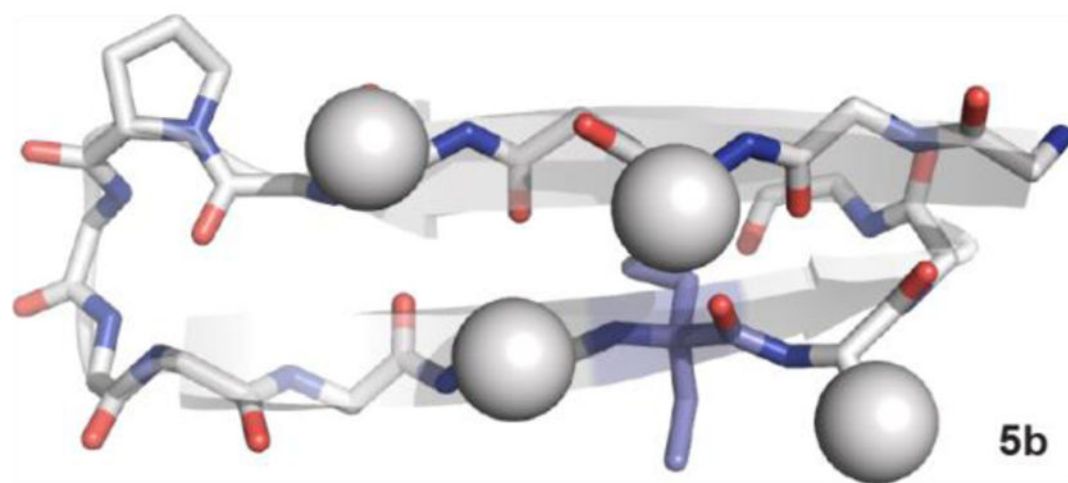
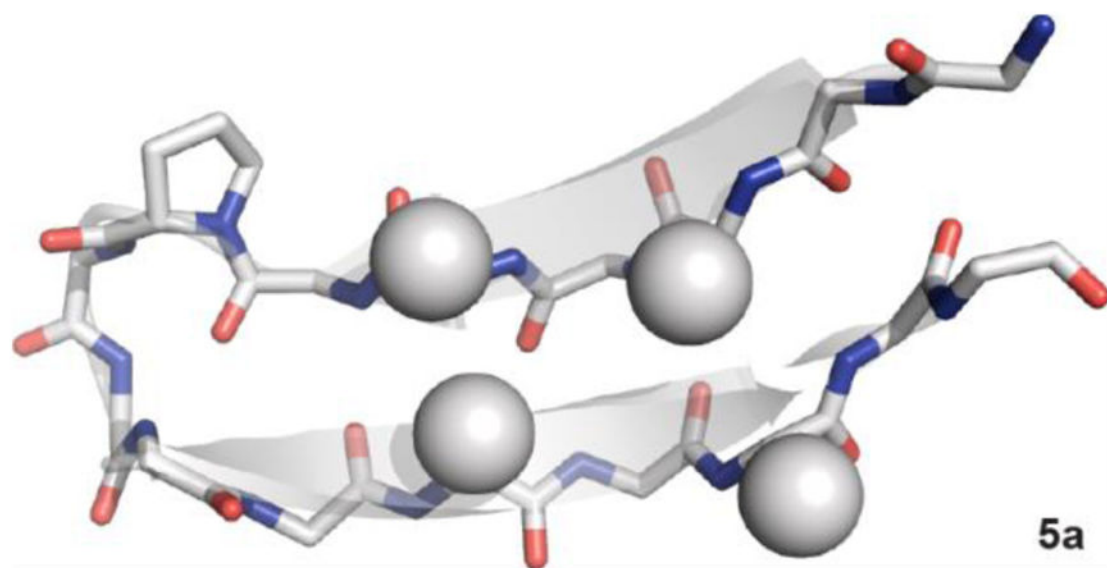


**Figure 4.** NMR structures of peptides **5a** and **5b**. Spheres represent the side-chains of hydrophobic core residues Trp<sup>3</sup>, Tyr<sup>5</sup>, Phe<sup>12</sup>, and Trp<sup>14</sup>. The  $\alpha,\alpha$ -dialkylated  $\alpha$ -amino acid in **5b** is colored purple.

**Table 1**Folding Thermodynamics of Peptides **1a–4a** at 278 K and Peptides **5a** and **1b–5b** at 298 K.

peptide	temperature (K)	$\delta_{\text{Gly10}}$ (ppm)	fraction folded <sup>a</sup>	$G_{\text{fold}}$ (kcal/mol) <sup>a</sup>
<b>1a</b>	278	0.202	$0.66 \pm 0.06$	$-0.4 \pm 0.1$
<b>2a</b>	278	0.201	$0.66 \pm 0.06$	$-0.4 \pm 0.1$
<b>3a</b>	278	0.208	$0.68 \pm 0.06$	$-0.4 \pm 0.1$
<b>4a</b>	278	0.209	$0.68 \pm 0.06$	$-0.4 \pm 0.1$
<b>1a<sup>b</sup></b>	293	0.185	$0.60 \pm 0.05$	$-0.2 \pm 0.1$
<b>1b</b>	298	0.026	$0.08 \pm 0.05$	$+1.41 \pm 0.04$
<b>2b</b>	298	0.080	$0.26 \pm 0.05$	$+0.6 \pm 0.1$
<b>3b</b>	298	0.083	$0.27 \pm 0.05$	$+0.6 \pm 0.1$
<b>4b</b>	298	0.091	$0.29 \pm 0.05$	$+0.5 \pm 0.2$
<b>5a</b>	298	0.310	$1.01 \pm 0.07$	N/A
<b>5b</b>	298	0.151	$0.49 \pm 0.05$	$+0.0 \pm 0.04$

<sup>a</sup>Error propagated assuming 0.010 ppm uncertainty in chemical shift assignments.<sup>b</sup>Previously reported at 293 K.<sup>20</sup> Included for comparison purposes.